Ocean Systems Engineering, *Vol. 3, No. 1 (2013) 035-053*
DOI: http://dx.doi.org/10.12989/ose.2013.3.1.035

Analytical study on hydrodynamic motions and structural behaviors of hybrid floating structure

Youn-Ju Jeong*, Du-Ho Lee, Min-Su Park and Young-Jun You

Infra-Structure Research Department, Korea Institute of Construction Technology
ilsan, Goyang, Gyeonggi 411-712, Korea

(Received February 22, 2013, Revised February 24, 2013, Accepted March 10, 2013)

Abstract. In this study, a hybrid floating structure with cylinder was introduced to reduce the hydrodynamic motions of the pontoon type. The hybrid floating structure is composed of cylinders and semi-opened side sections to penetrate the wave impact energy. In order to exactly investigate the hydrodynamic motions and structural behavior of the hybrid floating structure under the wave loadings, integrated analysis of hydrodynamic and structural behavior were carried out on the hybrid floating structure. Firstly, the hydrodynamic analyses were performed on the hybrid and pontoon models. Then, the wave-induced hydrodynamic pressures resulting from hydrodynamic analysis were directly mapped to the structural analysis model. And, finally, the structural analyses were carried out on the hybrid and pontoon models. As a result of this study, it was learned that the hybrid model of this study was showed to have more favorable hydrodynamic motions than the pontoon model. The surge motion was indicated even smaller motion at all over wave periods from 4.0 to 10.0 sec, and the heave and pitch motions indicated smaller motions beyond its wave period of 6.5 sec. However, the hybrid model was shown more unfavorable structural behavior than the pontoon model. High concentrated stress occurred at the bottom slab of the bow and stern part where the cylinder wall was connected to the bottom slab. Also, the hybrid model behaved with the elastic body motion due to weak stiffness of floating body and caused a large stress variation at the pure slab section between the cylinder walls. Hence, in order to overcome these problems, some alternatives which could be easily obtained from the simple modification of structural details were proposed.

Keywords: hybrid; floating structure; integrated analysis; motions; structural behavior; concrete; alternatives

1. Introduction

The floating structures of the pontoon type have been widely applied to offshore floating platforms because of many advantages of buoyancy, simple details, storage ability, and economy, etc (Allen *et al*. 2006, Haveman *et al*. 2006, Lanquetin *et al*. 2007). These offshore floating platforms such as container terminals, storage vessels, and LNG terminals are exposed to the severe offshore environment. Therefore, these offshore floating platforms should have high structural performance and low hydrodynamic motions to withstand the severe offshore environment during the service life (Link and Elwi 1995, Lanquetin *et al*. 2007).

*Corresponding author, Ph.D., E-mail: yjjeong@kict.re.kr

However, the floating structures of the pontoon type are unable to absorb wave impact energy due to the side sections not open to the wave action. Therefore, this system is vulnerable to the hydrodynamic motions. In order to satisfy design criteria for serviceability of the floating structures, it is required to have a large cross section and total weight (Jeong *et al*. 2010). Also, in order to expand the pontoon type's application to harsh offshore condition, it is very important to reduce the hydrodynamic motions of the pontoon type because unexpected hydrodynamic motions may cause uneasiness to people and breakdown to the facilities on the topside (Alexia *et al*. 2010, Clauss *et al*. 2009). With respect to the serviceability, among the six DOF (degree of freedom) of the hydrodynamic motions, vertical components of heave, pitch, and surge induced by vertical acceleration are important factors since the horizontal components are appropriately prevented by the mooring.

Also, these offshore floating platforms have been mainly constructed by the concrete (Pena *et al*. 2011, Lanquetin *et al*. 2007, Pham and Wang 2010). A floating concrete structure has a number of advantages, such as, low hydrodynamic motions, durability, and cost efficiency. However, considering the severe offshore environment and design characteristics of the concrete, such as, the higher tensile strength in the submerged parts to prevent cracking, it is very important to maintain certain level of structural performance for the floating concrete structures (Yao 2007, Pham and Wang 2010, Lanquetin *et al*. 2007). With respect to the structural performance, bending stress and high concentrated local stress by wave loadings are important factors.

In the design process of the floating concrete structures, it is required to evaluate the hydrodynamic motions and structural behavior under the wave loadings more precisely. The structural behavior of floating structures should be evaluated, including the effects of wave-induced hydrodynamic pressure subjected to the floating structures (Jeong and You 2011, Koutandos *et al*. 2004). However, there was a problem to exactly evaluate the structural behavior of floating structures since it was difficult to directly connect the wave-induced hydrodynamic pressure, resulting from the hydrodynamic analysis with the structural analysis model (Lee and Jeong 2011).

In this study, the hybrid floating structure with cylinder was introduced to reduce the hydrodynamic motions of the pontoon type (Park *et al.* 2010, 2012, Jeong *et al*. 2012). The hybrid floating structure is composed of cylinders and semi-opened side sections to penetrate the wave impact energy (Park *et al.* 2010 and 2012, Jeong *et al*. 2012). In order to investigate the hydrodynamic motions and structural behavior of the hybrid floating structure under the wave loadings, integrated analysis of hydrodynamic and structural behavior was carried out on the hybrid floating structures. Firstly, in order to investigate the hydrodynamic motions, hydrodynamic analyses were performed on the hybrid and pontoon models and the hydrodynamic motions of heave, pitch, and surge were analyzed. Then, in order to simulate real structural behavior of floating body under the wave loadings, wave-induced hydrodynamic pressures resulting from the hydrodynamic analysis were directly mapped to the structural analysis model. Finally, the structural analyses were carried out on the hybrid and pontoon models and the structural behavior of stress and deformation were analyzed.

2. Integrated analysis of hydrodynamic and structural behavior

2.1 Integrated analysis method

In order to investigate the hydrodynamic motions and structural behavior of the hybrid floating structure with cylinders, the integrated analysis of the hydrodynamic and structural behavior was carried out on the hybrid floating structures. The process of integrated analysis was provided on Fig. 1. The integrated analysis of this study is able to exactly evaluate structural behavior of the floating structures under the wave loadings since this method may directly reflect the wave-induced hydrodynamic pressure resulting from the hydrodynamic analysis to the structural analysis model (Lee and Jeong 2011).

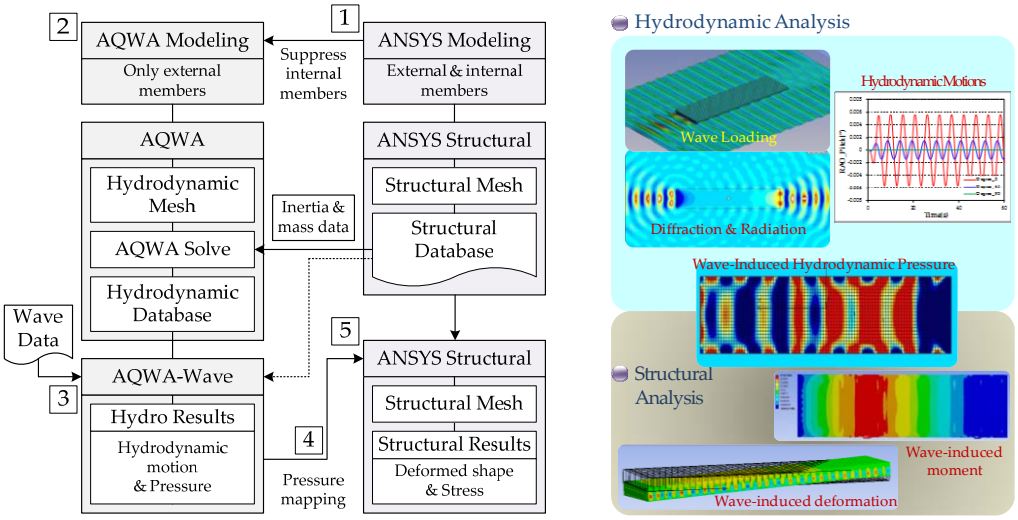

Fig. 1 Flowchart of the integrated analysis of hydrodynamic and structural analyses

First, in order to investigate the hydrodynamic motions, the hydrodynamic analyses using AQWA (ANSYS 2010, Palo 2005, Clauss *et al*. 2009) were performed on the hybrid and pontoon models and the hydrodynamic motions of heave, pitch, and surge were analyzed. Then, in order to simulate real structural behavior of floating body under the wave loadings, the wave-induced hydrodynamic pressures resulting from hydrodynamic analysis (AQWA) were directly mapped to the structural analysis model (ANSYS) by using Workbench Interface of ANSYS Inc, (ANSYS 2010). Finally, the structural analyses using ANSYS were carried out on the hybrid and pontoon models, where the mapped wave-induced hydrodynamic pressures were applied on the floating body with external forces, and structural behavior of stress and deformation were analyzed.

2.2 Analysis models

In this study, the hybrid floating structure with cylinder was introduced to reduce the hydrodynamic motions of the pontoon type (Park *et al.* 2010, 2012, Jeong *et al*. 2012). The hybrid floating structure is composed of cylinders and semi-opened side sections to penetrate the wave impact energy, as indicated in Fig. 2(b). The hybrid model was designed to have mixed structural shape of the pontoon type having high structural strength and the semi-submergible type having absorb-ability of wave impact energy. The sizes of the FE models were 120 m (length) × 90 m

(width) × 14 m (height). The drafts were 10.2 m and total weights were 38,112 ton for both models of the hybrid and pontoon. The cylinder diameter and air-gap distance of hybrid model were 20.0 and 10.0 m, respectively.

Material properties and details of the FE models were given in Table 1. The hydrodynamic motions of the floating body may be influenced by total weight and draft of floating body. Therefore, in order to evaluate the hydrodynamic motion of the hybrid model only in term of floating body shape, total weight (38,112 ton) and draft (10.2 m) of the hybrid model were manually set to the same with the pontoon model in hydrodynamic analysis. However, in order to evaluate structural behavior of the hybrid model in real structural stiffness, the details of the hybrid model were set to the same dimension with the real geometry, as indicated in Table 1, in structural analysis.

The ocean conditions of 1,000 m (length) × 1,000 m (width) × 35 m (water depth) and twenty cases of wave loads ranging from the wave period of 4.0 to 10.0 sec were selected for the hydrodynamic analysis. Also, in order to investigate the influence of incident wave (β) on the hydrodynamic motions and structural behavior, three cases of incident wave of 0°, 45°, and 90° were selected, as shown in Fig. 3. In this study, in order to investigate the free hydrodynamic motions of the models, the mooring system was not applied to the FE models.

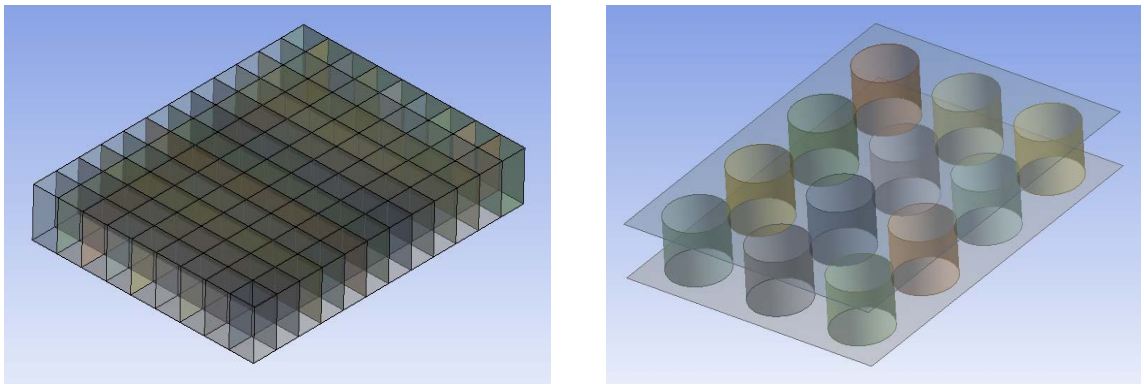

(a) Pontoon Model (b) Hybrid Model

Fig. 2 Analysis model

Table 1 Details and material properties of the floating structure

Details of the hybrid model		Details of the pontoon model		Concrete material properties	
Slab thickness	0.65 m	Slab thickness	0.65 m	Compressive strength	40.0 MPa
Cylinder wall thickness	0.65 m	External wall thickness	0.65 m	Tensile strength	4.0 MPa
Cylinder diameter	20.0 m	Internal wall thickness	0.30 m	Unit weight	24 kN/m^2
Cylinder interval	10.0 m	Internal wall interval	10.0 m	Elastic coefficient	33,935 MPa

3. Hydrodynamic motions of hybrid model

The hydrodynamic motion equation of the floating body can be expressed as follows and the hydrodynamic motions, $X(\omega)$ of the floating body under the wave loadings, can be calculated from Eq. (1) (Choi *et al*. 2011, Park *et al*. 2012).

$$\left[-\omega^2\left(M_s + M_a(\omega)\right) - i\omega C(\omega) + K\right]X(\omega) = F(\omega) \tag{1}$$

Where M_s is the inertia mass, $M_a(\omega)$ is the added mass by sea water, $C(\omega)$ is the radiation damping, K is the hydrostatic structural stiffness, $X(\omega)$ is the motions, and $F(\omega)$ is the excitation force from the wave loadings, respectively. Therefore, in order to investigate the hydrodynamic motions of the hybrid floating body, at first, excitation force, added mass, and radiation damping were calculated and the hydrodynamic motions of the surge, heave, and pitch were compared with the pontoon model.

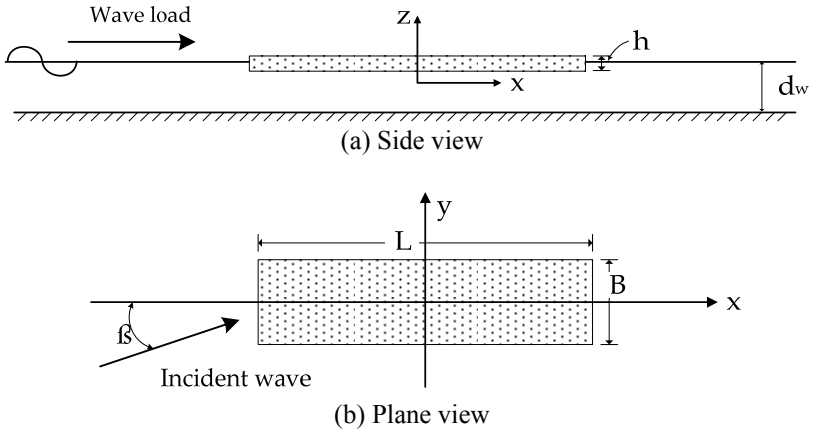

Fig. 3 Incident wave of the hydrodynamic analysis

3.1 Excitation forces

As a result of the hydrodynamic analysis, excitation forces of the hybrid model according to two cases of incident wave loadings of 0° and 45° were provided in Figs. 4 and 5, respectively. The surge, heave, and pitch excitation forces of the hybrid model at the incident wave of 0° were provided in Fig. 4. The hybrid model of this study indicated even smaller surge excitation force beyond the wave period of 5.0 sec. Also, the hybrid model indicated smaller heave and pitch excitation forces between the wave period of 6.5 sec and 8.5 sec than the pontoon model, although it presented little larger excitation forces at the below wave period of 6.5 sec. With respect to the peak excitation forces, whereas the excitation forces of the pontoon model gradually increased according to the increasing of wave periods, the hybrid model showed the peak surge and heave excitation forces at the wave period of 4.5 and 9.2 sec, respectively.

The surge, heave, and pitch excitation forces of the hybrid model at the incident wave of 45°

were provided in Fig. 5. The excitation forces of the hybrid model showed a different pattern with the incident wave of 0°. The excitation forces of the hybrid model were shown even smaller surge, heave, and pitch excitation forces beyond the wave period of 7.0 sec.
With respect to the excitation forces, it was found that the air-gap effects of the hybrid model contributed to the decrease of the excitation forces due to the absorption of wave impact energy (Jeong and You 2011, Park *et al*. 2010). Also, decreasing effect of the excitation forces was significant in cases of the surge excitation forces and beyond the wave period of 6.5 sec.

3.2 Added mass by sea water

As a result of the hydrodynamic analysis, added mass by the sea water of the hybrid model was provided in Fig. 6. Added mass was the function of the shape of floating body, not dependent to the incident wave. Therefore, add mass was plotted to the wave periods.

Added mass for the surge force was provided in Fig. 6(a). Added mass for the surge force of the hybrid model was shown as the significant difference in all wave periods, ranging from 4.0 to 10.0 sec with the pontoon model, especially, shown in even greater difference at the short wave period ranging from 4.0 to 6.5 sec. Added mass for the heave force was provided in Fig. 6(b). Added mass for the heave force of the hybrid model indicated a similar pattern with the pontoon model in all wave periods ranging from 4.0 to 10.0 sec. Also, added mass for the heave force gradually decreased according to the increase in the wave periods for both models of hybrid and pontoon.

With respect to the added mass by the sea water, it was found that the water weight between the cylinders of the hybrid model contributed to increase added mass. Also, increase in effects of added mass was significant in cases of the surge term in all wave period ranging from 4.0 to 10.0 sec.

3.3 Radiation damping

As a result of the hydrodynamic analysis, the radiation damping of hybrid model was provided in Fig. 7. The radiation damping was also a function of the shape of the floating body, not dependent to the incident wave. Therefore, the radiation damping was plotted to the wave periods only.

The radiation damping for the surge force was provided in Fig. 7(a). The hybrid model of this study indicated a smaller surge radiation damping beyond the wave period of 5.0 sec, although indicated for even greater difference at the short wave period, ranging from 4.0 to 5.0 sec. The radiation damping for the heave force was provided in Fig. 7(b). The radiation damping for the heave force of the hybrid model indicated a similar pattern with the pontoon model all over the wave periods, ranging from 4.0 to 10.0 sec, although it was shown as a smaller radiation damping at the wave period, ranging from 6.5 to 9.0 sec.

With respect to the peak radiation damping, whereas the radiation damping of the pontoon model gradually increased according to the increasing of wave periods, the hybrid model indicated the peak radiation damping at the wave period of 4.5 and 9.2 sec for the surge and heave term, respectively. It was the same to the peak excitation forces at the incident wave of 0°

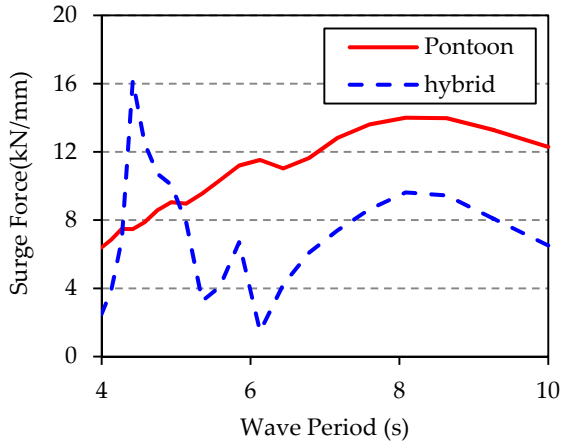

(a) Surge force, β=0°

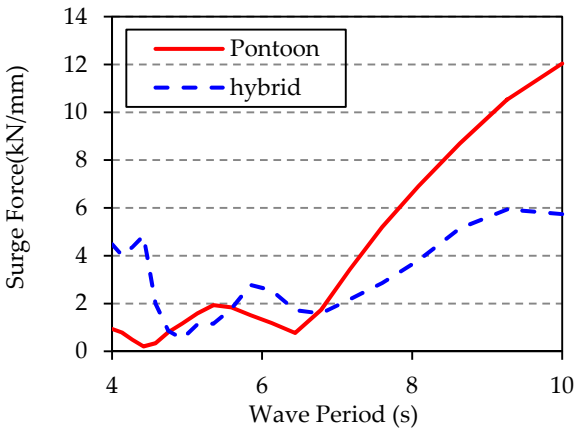

(a) Surge force, β=45°

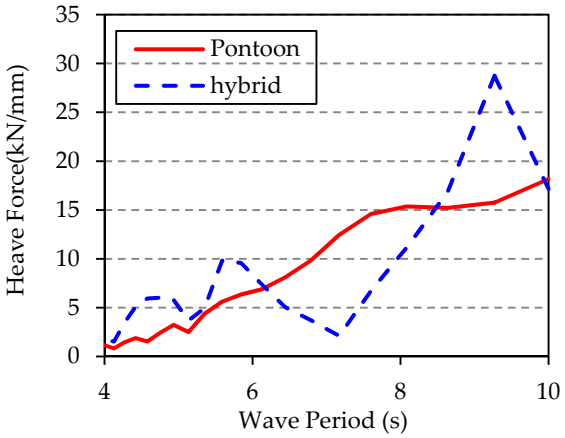

(b) Heave force, β=0°

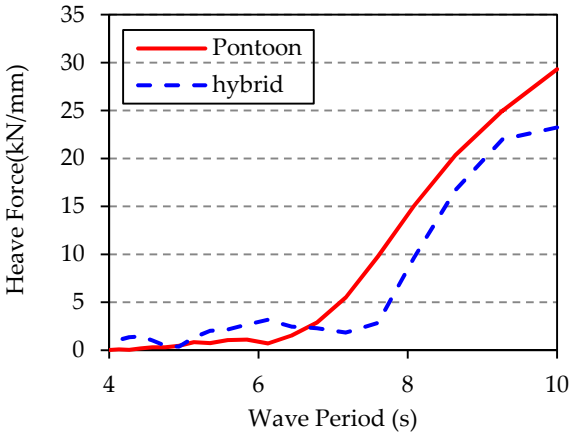

(b) Heave force, β=45°

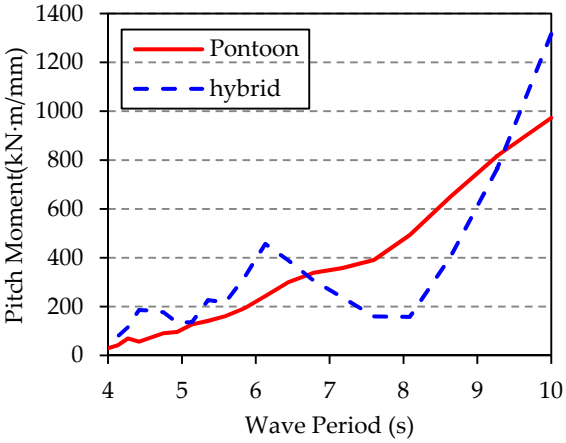

(c) Pitch moment, β=0°

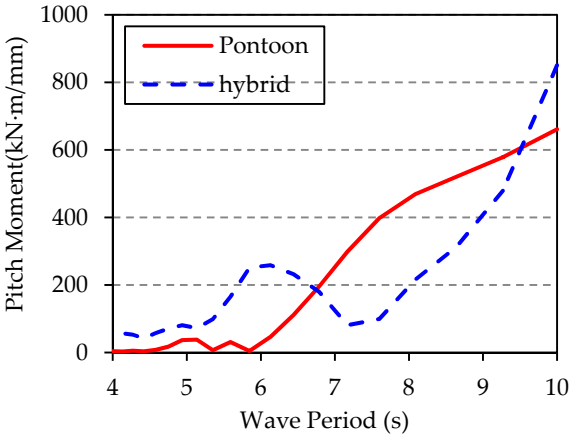

(c) Pitch moment, β=45°

Fig. 4 Excitation force at incident wave of 0°

Fig. 5 Excitation force at incident wave of 45°

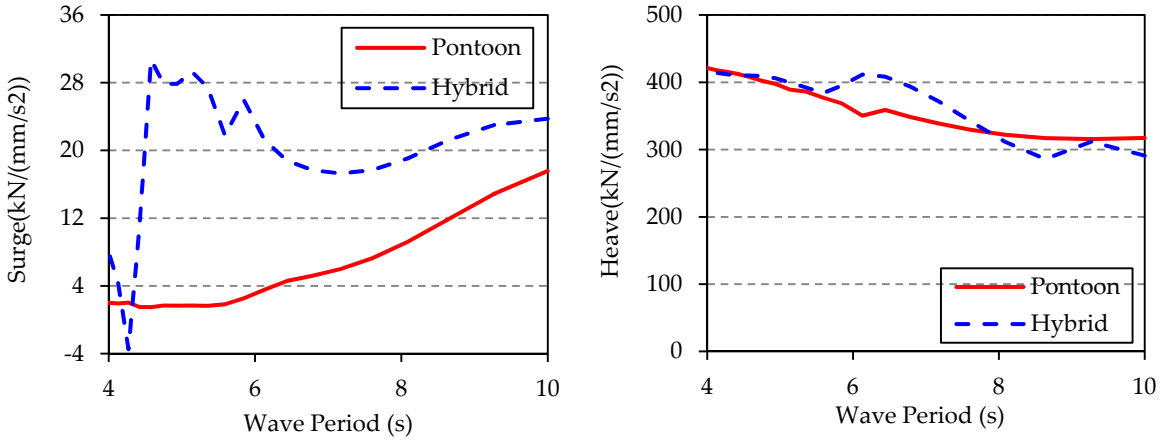

(a) Surge force (b) Heave force

Fig. 6 Added mass of the floating body

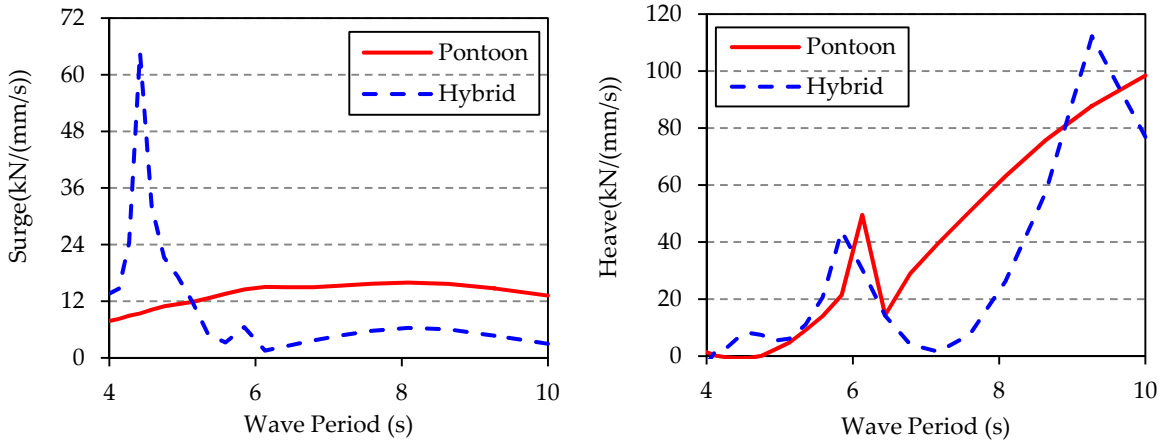

(a) Surge force (b) Heave force

Fig. 7 Radiation damping of the floating body

3.4 Hydrodynamic motions (RAOs)

As a result of the hydrodynamic analysis, the hydrodynamic motions of the hybrid model according to three cases of incident wave loadings of 0°, 45°, and 90° were provided in Figs. 8, 9, and 10, respectively. The surge, heave, and pitch motions of the hybrid model at the incident wave of 0° were provided in Fig. 8. The hybrid model of this study indicated even smaller surge motion at all wave periods, ranging from 4.0 to 10.0 sec. Also, the hybrid model indicated smaller heave and pitch motions beyond the wave period of 6.5 sec than the pontoon model. With respect to the

peak wave period, whereas the hybrid model indicated peak surge and pitch motions at the wave period of 9.0 and 10.0 sec, respectively, which was similar to the pontoon model, the peak heave motions were shown for the wave period 9.0 sec.

The surge, heave, and pitch motions of the hybrid model at the incident wave of 45° were provided in Fig. 9. Although the heave and pitch motions of the hybrid model indicated a similar pattern with the incident wave of 0°, which were indicated smaller heave and pitch motions beyond the wave period of 6.5 sec than the pontoon model, the surge motion presented different pattern with the incident wave of 0°. Whereas the hybrid model at the incident wave of 0° presented even smaller surge motion at all wave periods, ranging from 4.0 to 10.0 sec, the hybrid model at the incident wave of 45° indicated a similar surge motion with the pontoon model.

The sway, heave, and roll motions of the hybrid model at the incident wave of 90° were provided in Fig. 10. The hydrodynamic motions of the hybrid model presented a similar pattern with the incident wave of 0°. These were indicated even smaller sway motion at all wave period, ranging from 4.0 to 10.0 sec, and indicated smaller heave and roll motions beyond the wave period of 6.5 sec than the pontoon model. Whereas the hybrid model indicated peak sway motion at the wave period of 8.5 sec, which was similar to the pontoon model, peak pitch motion indicated at the wave period of 9.2 sec.

Summarizing the hydrodynamic motions, the hybrid model of this study indicated more favorable hydrodynamic motions than the pontoon model. The surge motion indicated even smaller motion at all wave periods, ranging from 4.0 to 10.0 sec, and the heave and pitch motions indicated smaller motions beyond the wave period of 6.5 sec where is more unfavorable to the serviceability and structural safety of the floating body than the short wave period below 6.5 sec.

4. Structural behavior of hybrid model

4.1 Structural analysis using wave-induced hydrodynamic pressure

The structural behavior of the floating structures should be evaluated by including the effect of wave-induced hydrodynamic pressure subject to the floating structures. However, there has been a problem to exactly evaluate the structural behavior of the floating structures since it was difficult to directly connect with the wave-induced hydrodynamic pressure resulting from the hydrodynamic analysis with the structural analysis model. In this study, in order to exactly evaluate the structural behavior of the floating structures under the wave loadings, the integrated analysis of the hydrodynamic motions and the structural behavior was carried out to the hybrid and pontoon models. The wave-induced hydrodynamic pressures resulting from the hydrodynamic analysis (AQWA) were directly mapped to structural analysis model (ANSYS) by using Workbench Interface of ANSYS Inc, (ANSYS 2010, Lee and Jeong 2012). The wave-induced hydrodynamic pressure corresponding to the wave period of 10.0 sec was selected for the structural analysis, as occurred for the maximum hydrodynamic motions for all incidence waves.

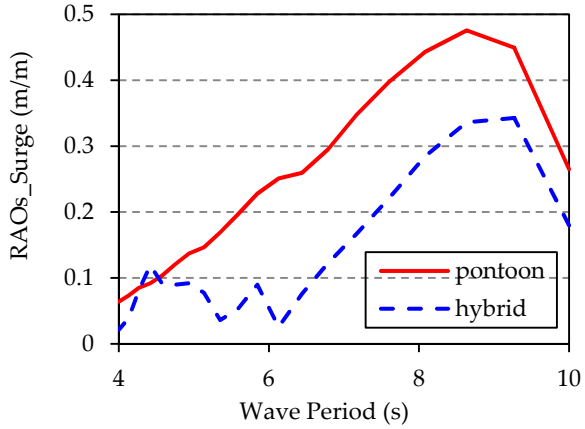

(a) Surge RAOs, β=0°

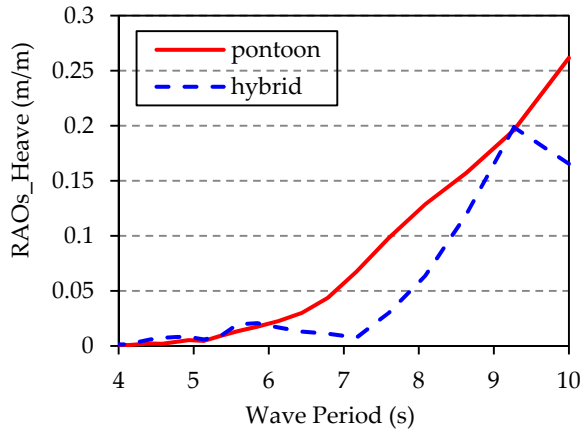

(b) Heave RAOs, β=0°

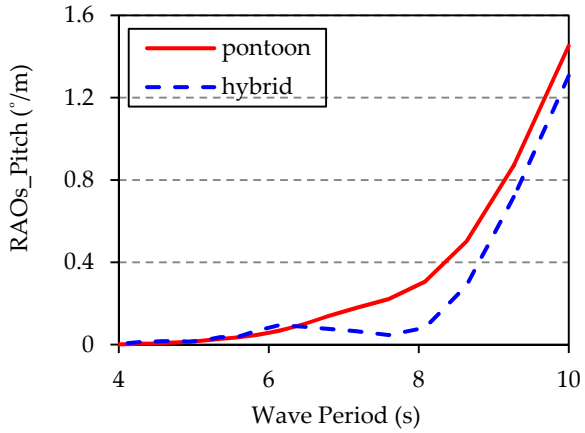

(c) Pitch RAOs, β=0°

Fig. 8 RAOs at Incident Wave of 0°

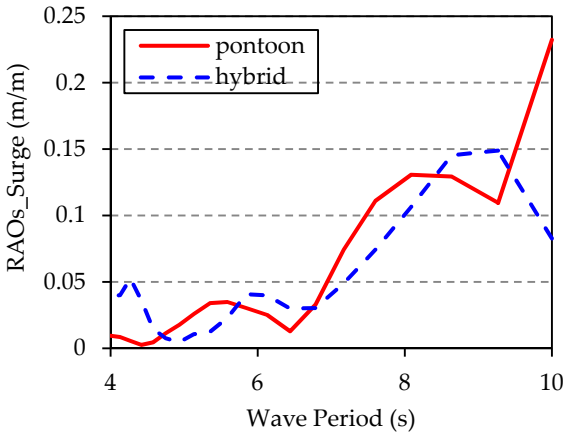

(a) Surge RAOs, β=45°

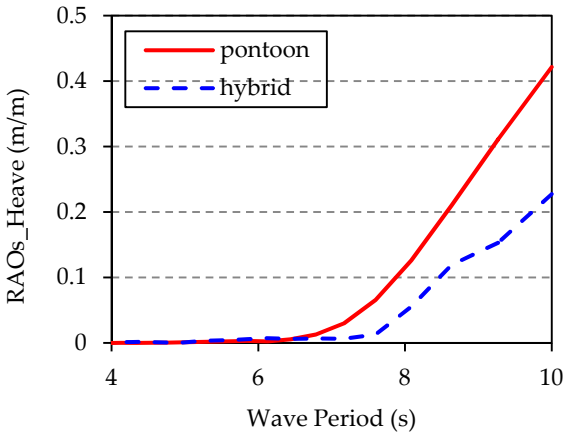

(b) Heave RAOs, β=45°

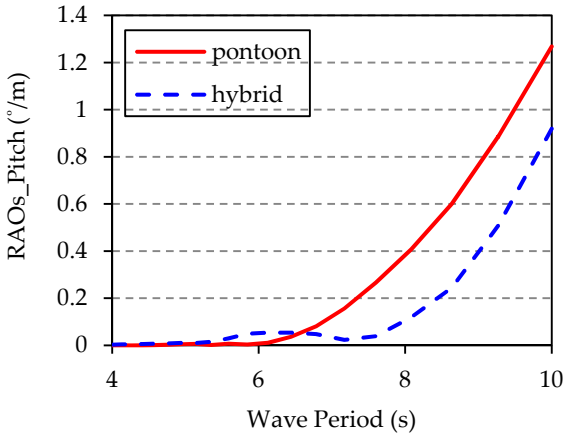

(c) Pitch RAOs, β=45°

Fig. 9 RAOs at Incident Wave of 45°

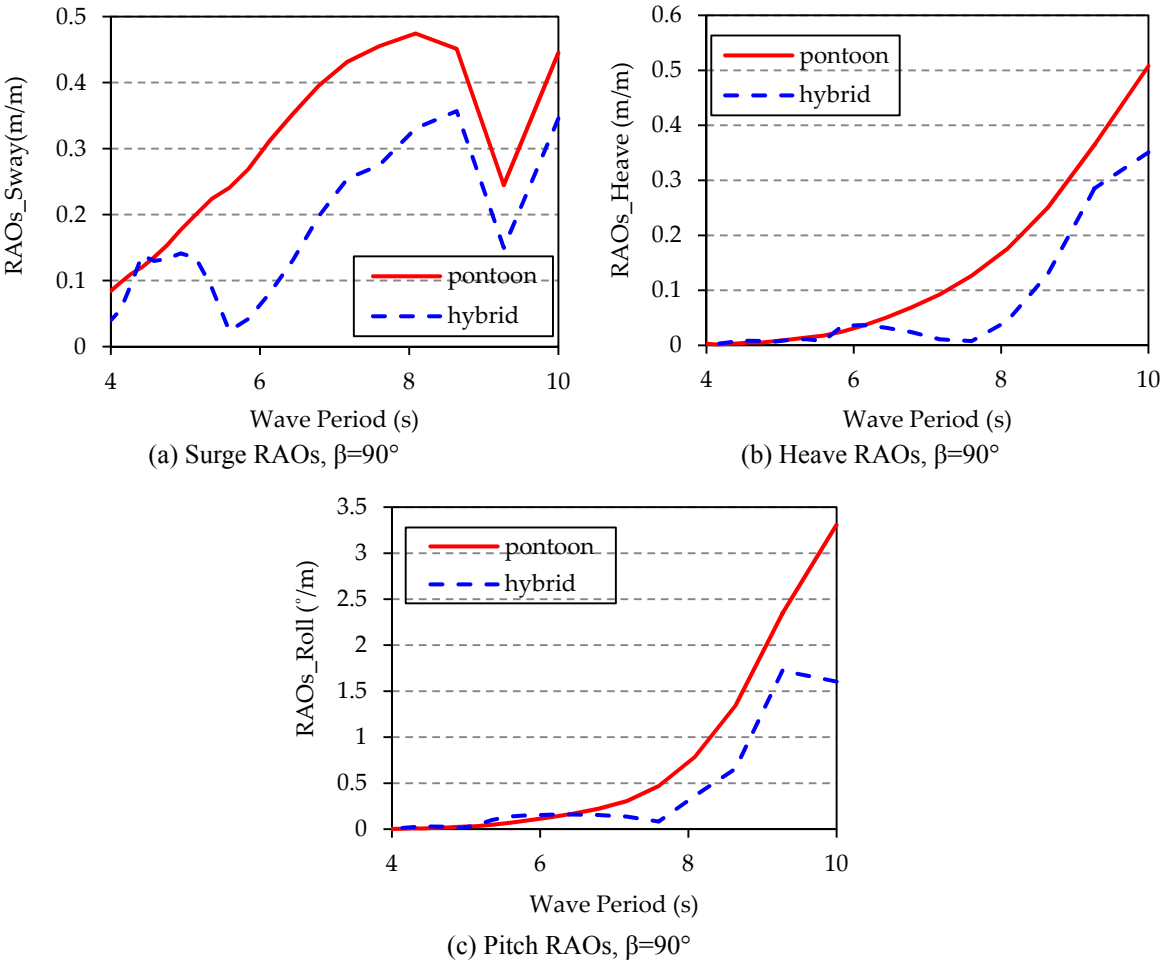

(a) Surge RAOs, β=90°

(b) Heave RAOs, β=90°

(c) Pitch RAOs, β=90°

Fig. 10 RAOs at Incident Wave of 90°

4.2 Structural behavior under wave loadings

As a result of the structural analysis, the structural stress contours of the bottom slab according to three cases of incident waves of 0°, 45°, and 90° were provided in Figs. 11 and 12 for the pontoon and hybrid models, respectively. The structural behaviors of the bottom slab of the pontoon model indicated similar pattern with the incident wave direction, as presented in Fig. 11. In cases of the incident waves of 0° and 90°, the stresses of the bottom slab were distributed nearly symmetric patterns to the longitudinal and transverse axis, respectively. Also, in case of the incident wave of 45°, the stress of the bottom slab was distributed to the symmetric pattern to the diagonal axis, where the higher stress occurred at the longitudinal right bottom side than the left upper side.

The structural behaviors of the bottom slab of the hybrid model indicated a similar pattern with

the incident wave direction for two cases of the incident waves of 0° and 90°, as presented in Figs. 12(a) and (c), respectively. However, the symmetric patterns of the stress became even looser than the pontoon model. In case of the incident wave of 45°, it was difficult to confirm the symmetry of the stress level to the diagonal axis. Also, a high stress at the longitudinal right bottom side as occurred at the pontoon model did not appear. It may be attributed to the fact that these types of phenomenon for the hybrid model were caused by wave interaction between the cylinders (Park *et al*. 2010) and the absorption of wave impact energy through the air-gap.

In most cases, the high concentrated stress occurred at the bow part directly subject to the incident wave loadings (Huang and Moan 2005, Koutandos *et al*. 2004, Jeong and You 2011), as presented in Figs. 11 and 12. However, in case of the hybrid model with the incident wave of 90°, the high concentrated stress occurred at the stern part, as presented in Fig. 12(c).

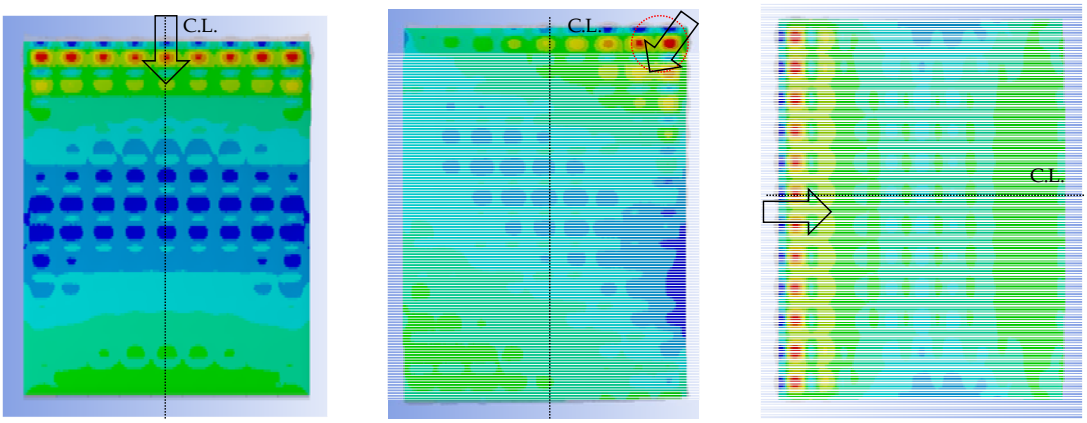

(a) Incident wave of 0° (b) Incident wave of 45° (c) Incident wave of 90°

Fig. 11 Stress contour of the bottom slab of the pontoon models

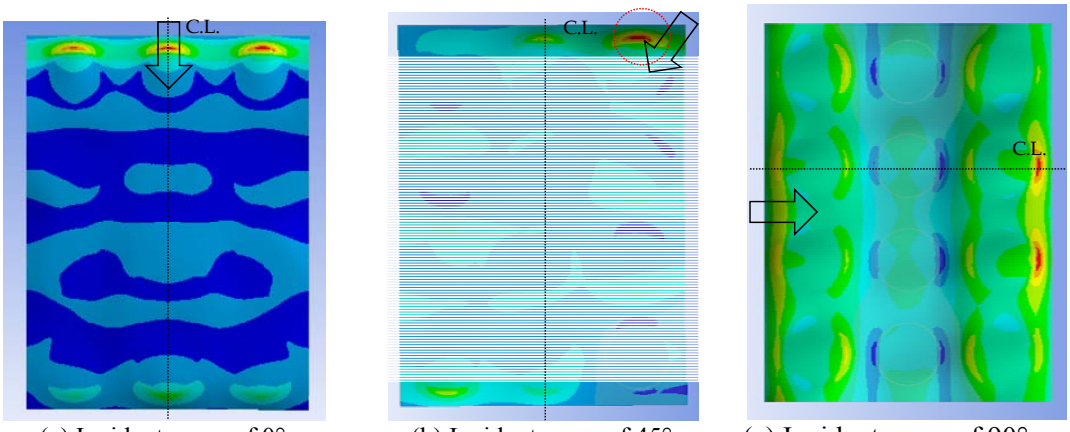

(a) Incident wave of 0° (b) Incident wave of 45° (c) Incident wave of 90°

Fig. 12 Stress contour of the bottom slab of the hybrid models

Also, the structural stress contours of the side wall according to three cases of incident waves of 0°, 45°, and 90° were provided in Figs. 13 and 14 for the pontoon and hybrid models, respectively. In most cases, the high concentrated stress occurred at the bow part directly subject to the incident wave loading (Huang and Moan 2005, Koutandos *et al*. 2004, Jeong and You 2011), as presented in Figs. 13 and 14. However, in case of the hybrid model with the incident wave of 90°, the highly concentrated stress occurred at the stern part, as presented in Fig. 12(c).

In cases of the pontoon model, the maximum stresses of side wall occurred at the mid span of side walls, where the internal walls were located at both ends. However, in cases of the hybrid model, the maximum stresses of side wall occurred at the bottom edge of cylinder, where cylinder walls were connected to the bottom slab.

It was mainly caused by the "cantilever effect" at the edge of the bottom slab of the hybrid model. The bottom slab of the hybrid model has 50 mm of the cantilever arm length from the cylinder outside. Therefore, according to the hydrodynamic motions of heave and pitch, the vertical buoyancy force was locally subject to the edge of the bottom slab and the high concentrated stress occurred at the connection part of the cylinder wall and bottom slab, as presented in Fig. 15. Another reason was the "wave run-up phenomenon". At the bow part, wave loadings were subject to the upward direction and this wave run-up loading was subject to the edge of the bottom slab and increased local stress.

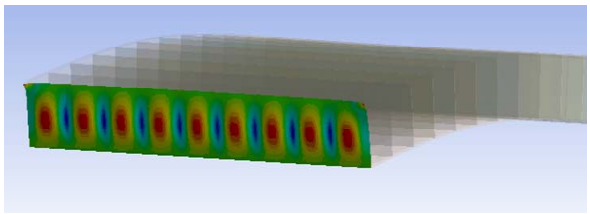

(a) Incident wave of 0°

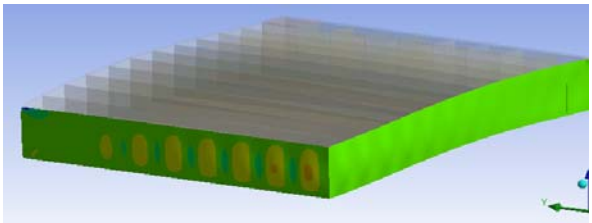

(b) Incident wave of 45°

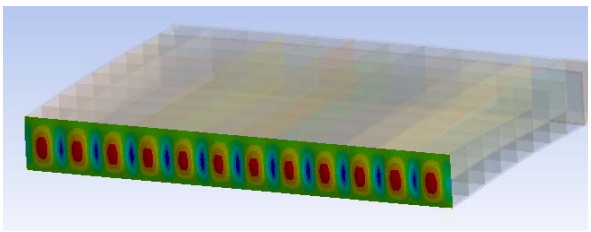

(c) Incident wave of 90°

Fig.13 Stress contour of the side wall of the pontoon models

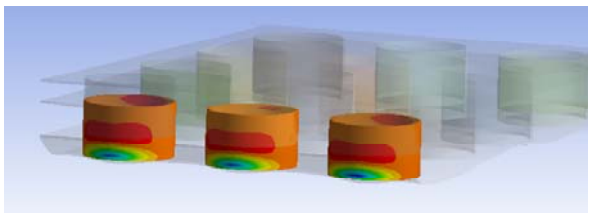

(a) Incident wave of 0°

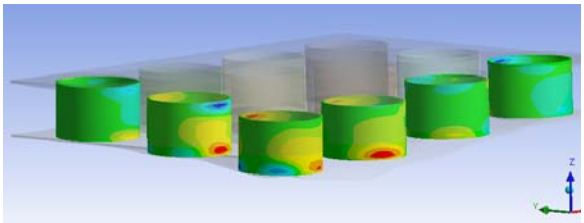

(b) Incident wave of 45°

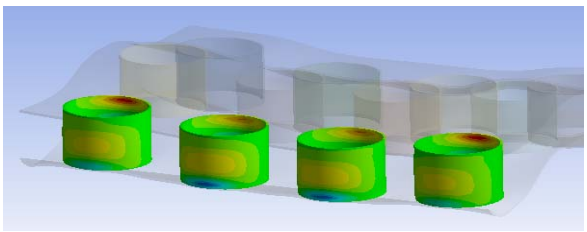

(c) Incident wave of 90°

Fig. 14 Stress contour of the cylinder wall of the hybrid models

4.3 Stress distribution at bottom slab

In order to investigate the stress distribution and stress level, the stresses of bottom slab were plotted along the floating body length according to three cases of incident waves of 0°, 45°, and 90°, as provided in Fig. 16, respectively. As a result of the stress distribution, it was learned that the pontoon model behaved with the rigid body motion, as presented in Fig. 13. Although the hydrodynamic motions of the pontoon model were larger than the hybrid model, the stress levels were insignificant for three cases of incident waves, as presented in Fig. 16. It was caused by strong stiffness of the pontoon model. The interior part of the pontoon model was consisted of many internal walls and these internal walls sufficiently resisted to the bending moment due to the wave loadings.

However, it was found that the hybrid model behaved with the elastic body motion, as presented in Fig. 14. Although the hydrodynamic motions of hybrid model were smaller than the pontoon model, the stress levels were larger than the pontoon model for three cases of incident waves, as presented in Fig. 16. It was caused by weak stiffness of the hybrid model (Kim 2011). Although the interior part of the hybrid model was consisted of some cylinder walls, it was learned that it was too weak to resist the bending moment due to the wave loadings. Stresses at the pure slab section between the cylinders changed drastically due to the weak stiffness, as presented in Fig. 16. Especially, the high concentrated stress occurred at the bow and stern part of the bottom slab of the hybrid model, where cylinder wall was connected to the bottom slab, due to the "cantilever effect" and "wave run-up phenomenon" of the bottom slab. Whereas the stress level of the pontoon model satisfied the concrete tensile strength of 4.0 MPa for three cases of incident waves, the stress levels of hybrid model were over the concrete tensile strength at the bow and stern part.

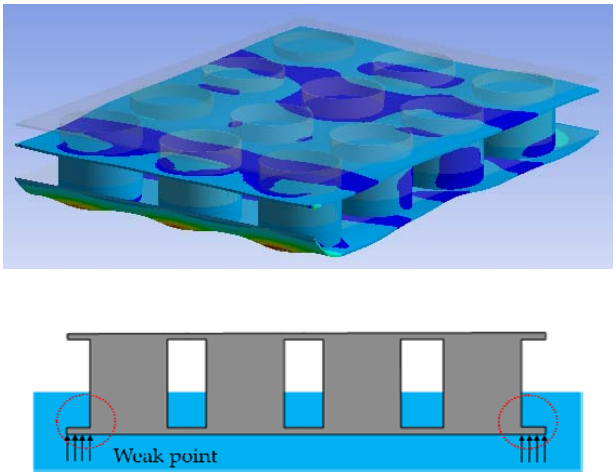

Fig. 15 Cantilever effect at the edge of the bottom slab

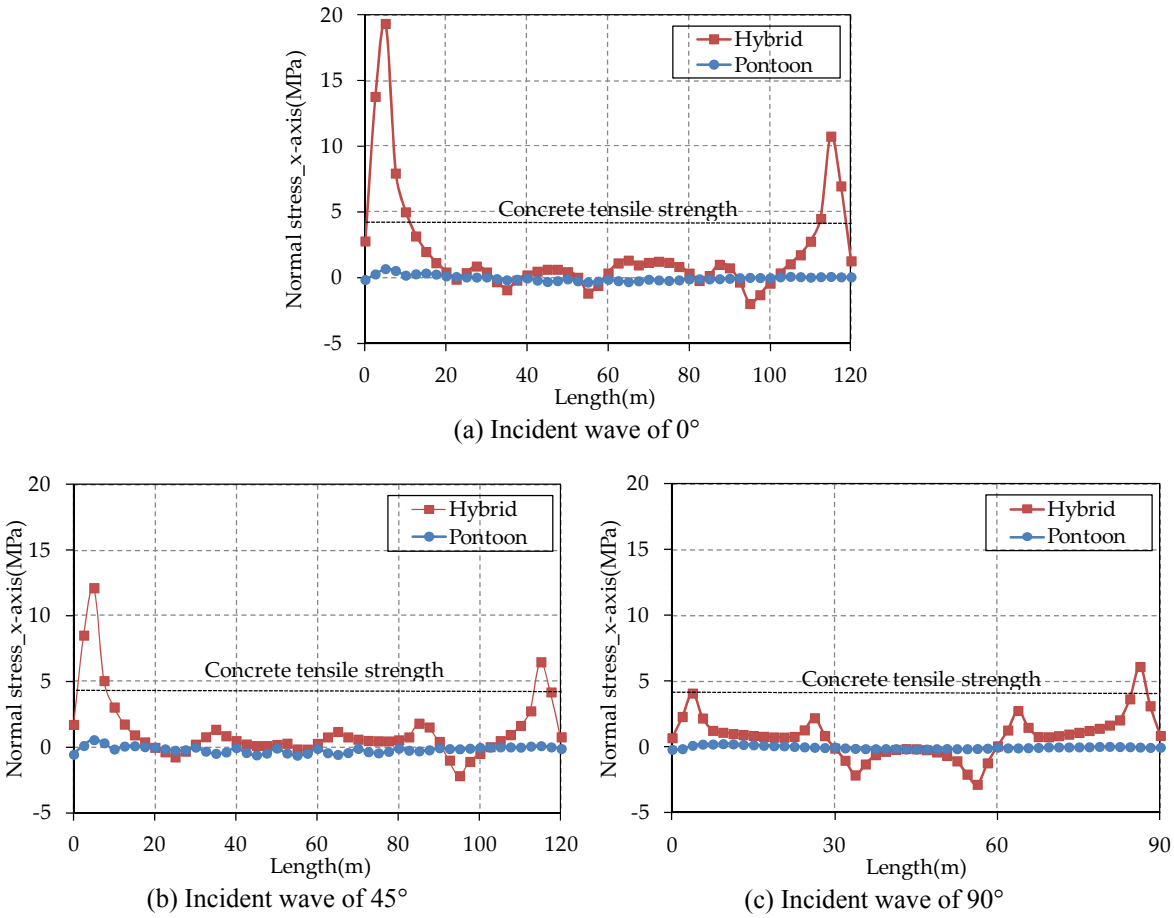

(a) Incident wave of 0°

(b) Incident wave of 45°

(c) Incident wave of 90°

Fig. 16 Stress distribution of the bottom slab

4.4 Alternatives for structural performance

As a result of the structural behavior investigation, there were two problems for the structural performance of hybrid model in this study. The first problem was that the hybrid model behaved with elastic body motion due to the weak stiffness of floating body and caused a large stress variation at the pure slab section between the cylinder walls. And, the second problem was that a high concentrated stress occurred at the edge of the bottom slab of the bow and stern part, where cylinder wall was connected to the bottom slab.

The first problem can be overcome partially by installing a hunch at the top and bottom of cylinder walls, as indicated in Fig. 17. The hunch parts at the top and bottom of cylinder walls were not modeled in this study for the purpose of improving efficiency of the hydrodynamic analysis and structural analysis. According to this alternative, the stiffness of internal slab section should be improved. Therefore, this alternative should be contributed to reduce the elastic body motion and to resist the bending moment under the wave loadings, resulting from reducing a large

stress variation at the pure slab section between the cylinders, as presented in Fig. 17(c). Also, this alternative should be contributed to overcome the second problem.

Other alternatives to overcome this problem are installing the stiffeners onto the top and bottom slabs to connect both cylinders or to combine the hybrid type with the pontoon type as to improve both hydrodynamic motions and structural performance, as presented in Fig. 18. Also, these alternatives should be contributed to reduce the elastic body motion and resist the bending moment under the wave loadings resulting from improving stiffness at the pure slab section between the cylinders.

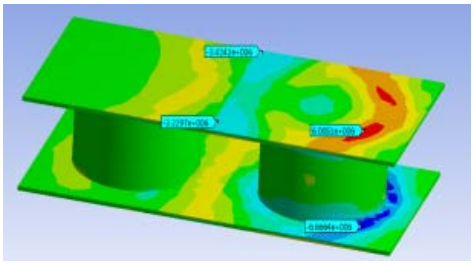

(a) No hunch edge

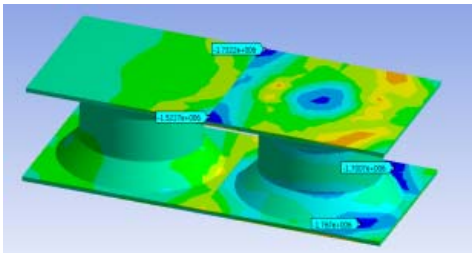

(b) Hunch edge

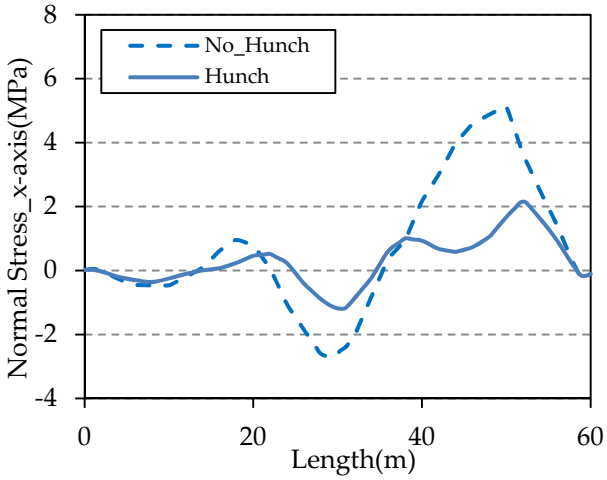

(c) Hunch effect on stress

Fig. 17 Hunch effects on the slab stress

The second problem may be overcome by installing cylinder walls at the end of the bottom slab, as presented in Fig. 19. According to this alternative, outside bottom slab from the cylinder walls should be removed. Therefore, this alternative should be contributed to reduce a high concentrated stress at the edge of the bottom slab of the bow and stern parts resulting from removing the "cantilever effects" and reducing the "wave run-up phenomenon".

Summarizing the structural behavior of a hybrid model, the hybrid model of this study showed more unfavorable structural behavior than the pontoon model. Whereas the stress levels of the

pontoon model satisfied the concrete tensile strength of 4.0 MPa for three cases of incident waves, the stress levels of the hybrid model did not satisfy the concrete tensile strength at the bow and stern part. High concentrated stress occurred at the edge of the bottom slab of the bow and stern part, where cylinder wall was connected to the bottom slab, because of the "cantilever effects" and the "wave run-up phenomenon". Also, the hybrid model behaved with elastic body motion due to the weak stiffness of floating body and a caused large stress variation at the pure slab section between the cylinder walls. Therefore, some alternatives which may be easily obtained from simply modification of structural details were proposed to overcome these problems.

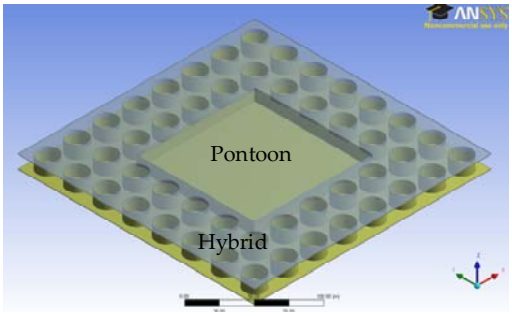

Fig. 18 Combine hybrid type with the pontoon type

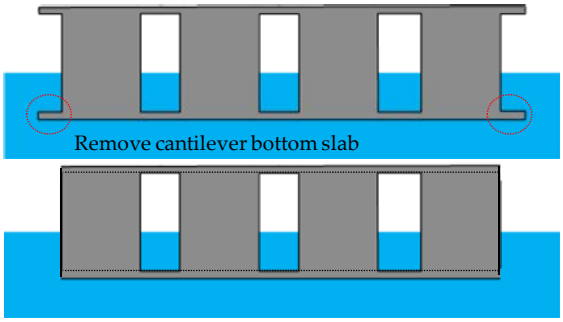

Fig. 19 Remove the Cantilever Bottom Slab

5. Conclusions

In this study, the hybrid floating structure with cylinder was introduced to reduce the hydrodynamic motions of the pontoon type. The hybrid floating structure is composed of cylinders and semi-opened side section to penetrate the wave impact energy. In order to investigate the hydrodynamic motions and structural behavior of the hybrid floating structure under the wave loadings, the integrated analysis of hydrodynamic and structural behavior were carried out on the hybrid floating structures. First, in order to investigate the hydrodynamic motions, the hydrodynamic analyses were performed on the hybrid and pontoon models and the hydrodynamic motions of heave, pitch, and surge were analyzed. Then, in order to simulate real structural behavior of floating body under the wave loadings, wave-induced hydrodynamic pressures resulting from the hydrodynamic analysis were directly mapped to the structural analysis model.

Finally, the structural analyses were carried out on the hybrid and pontoon models and the structural behavior of stress and deformation were analyzed.

As a result of this study, it was learned that the hybrid model of this study was shown more favorable hydrodynamic motions than the pontoon model. The surge motion indicated even smaller motion all over wave period from 4.0 sec to 10.0 sec and the heave and pitch motions shown smaller motions beyond the wave period of 6.5 sec where was more unfavorable to the serviceability and structural safety of the floating body than the short wave period below 6.5 sec.

However, the hybrid model of this study shown more unfavorable structural behavior than the pontoon model. Whereas the stress levels of the pontoon model satisfied the concrete tensile strength of 4.0 MPa for three cases of incident waves, the stress levels of the hybrid model did not satisfy the concrete tensile strength at the bow and stern parts. High concentrated stress occurred at the edge of the bottom slab of the bow and stern parts where cylinder wall was connected to the bottom slab, because of the "cantilever effects" and "wave run-up phenomenon". Also, the hybrid model behaved with elastic body motion due to the weak stiffness of the floating body and caused a large stress variation at the pure slab section between the cylinder walls. Therefore, some alternatives which can be easily obtained from a simply modification of structural details are proposed to overcome these problems.

Acknowledgments

This study was supported by the Korea Institute of Construction Technology through the research project, named "Development of construction technology for concrete floated offshore infrastructures"

References

Alexia, A., Wendy, S.R., Dominique, R., Patri, F. and Wayne, G. (2010), "Feability and design of the clubstead: a cable-stayed floating structure for offshore dwellings", *Proceedings of the 29th International Conference on Ocean, Offshore and Arctic Engineering: OMAE2010-20268*, Shanghai, China.

Allen, E., Dees, D., Hicks, S., Hollibaugh, R., Martin, T. and Starling, T. (2006), *Design of a floating production storage and offloading vessel for offshore Indonesia-final report*, Texas A&M University.

ANSYS (2010), *ANSYS AQWA User's Manual*, ANSYS Inc. PA.

Cheetham, P., Du, S., May, R. and Smith, S. (2007), "Hydrodynamic analysis of ships side by side in waves", *Proceedings of the International Aerospace CFD Conference*, Paris, France.

Choi, Y.R., Hong, S.Y., and Choi, H.S. (2011), "An analysis of second-order wave forces on floating bodies by using higher-order boundary element method", *Ocean Eng.*, **28**(1), 117-138.

Clauss, G.F., Sprenger, F., Testa, D., Hoog, S. and Huhn, R. (2009), "Motion behaviour of a new offshore LNG transfer system at harsh operational conditions", *Proceedings of the 28th International Conference on Ocean, Offshore and Arctic Engineering: OMAE2009-79391*, Honolulu, USA.

Haveman, C., Parliament, J., Sokol, J., Swenson, J. and Wangner, T. (2006), *Design of a Floating Production Storage and Offloading Vessel for Operation in the South China Sea-Final Report*, Texas A&M University.

Huang, W. and Moan, T. (2005), "Combination of global still-water and wave load effects for reliability-based design of floating production, storage and offloading (FPSO) Vessels", *Appl. Ocean Res.*, **27**, 127-141.

Jeong, Y.J., Cho, J.Y., You, Y.J. and Na, S.W. (2010), "Stability and wave-induced bending moment for design of offshore floating terminal", *Proceedings of the 9th Pacific Structural Steel Conference 2010*, Beijing, China, 369-374.

Jeong, Y.J., Lee, D.H., Park, M.S. and You, Y.J. (2012), "Hydrodynamic and oscillatory motions of hybrid floating structures with cylinders", *Proceedings of the IEEE-OCEANS2012: OCEANS120612-002*, Virginia Beach, USA.

Jeong, Y.J. and You, Y.J. (2011), "Experimental study for wave-induced hydrodynamic pressure subjected to bottom of floating structures", *Proceedings of the IEEE-OCEANS 2011*, Santander, Spain.

Kim, K.T. (2011), *Hydroelastic Analysis of Three Dimensional Floating Structures*, MS.c. Thesis, KAIST, Korea.

Koutandos, E.V., Karambas, T.V. and Koutitas, C.G. (2004), "Floating breakwater response to waves action using a boussinesq model coupled with a 2D velliptic solver", *J. Waterway Port. Coastal, Ocean Eng. - ASCE*, **130**(5), 243-255.

Lanquetin, B., Collet, P. and Esteve, J. (2007), "Structural integrity management for a large prestressed concrete floating production unit", *Proceedings of the 26th International Conference on Offshore Mechanics and Arctic Engineering: OMAE2007-29535*, San Diego, USA.

Lee, D.H. and Jeong, Y.J. (2011), "Integrated analysis of hydrodynamic motions and structural behavior of large-scaled floating structures using AQWA-ANSYS coupling (In Korean)", *Comput. Struct. Eng. Korea*, **130**, 243-255.

Link, R.A. and Elwi, A.E. (1995), "Composite concrete-steel plate walls: analysis and behavior", *J. Struct. Eng. - ASCE*, **121**(2), 260-271.

Palo, P. (2005), "Mobile offshore base: hydrodynamic advancements and remaining challenges", *Mar. Struct.*, **18**(2), 133-147.

Park, M.S., Koo, W.C. and Choi, Y.R. (2010), "Hydrodynamic interaction with an array of porous circular cylinders", *Int. J. Naval Architect. Ocean Eng.*, **2**(3), 146-154.

Park, M.S., Koo, W.C. and Kawana, K. (2012), "Numerical analysis of the dynamic response of an offshore platform with a pile-soil foundation system subjected to random waves and currents", *J. Waterway Port. Coastal. Ocean Eng. - ASCE*, **138**(4), 275-285.

Pena, E., Ferreras, J. and Sanchez-Tembleque, F. (2011), "Experimental study on wave transmission coefficient, mooring lines and module connector forces with different designs of floating breakwaters", *Ocean Eng.*, **38**(10), 1150-1160.

Pham, D.C. and Wang, C.M. (2010), "Optimal layout of gill cells for very large floating structures", *J. Struct. Eng. - ASCE*, **136**(7), 907-916.

Yao, Z. (2007), *Very Large Floating Container Terminal and Optimal Layout of GillCells,* MS.c. Thesis, National University of Singapore.

This work was presented in CODE 2012 on November 13-16, 2012, Jeju, Korea.
(The 2nd International Conference in Computational Design in Engineering)